Long non-coding RNA CRNDE may be associated with poor prognosis by promoting proliferation and inhibiting apoptosis of cervical cancer cells through targeting PI3K/AKT

H. Y. YANG, C. P. HUANG*, M. M. CAO, Y. F. WANG, Y. LIU

Gynecological Clinic, Second Hospital of Shandong University, Jinan, Shandong, China

Correspondence: cuipinghuang3102@sina.com

Long non-coding RNAs (lncRNAs) are attracting more and more attention from researchers because they are relatively new factors in regulating biological processes in human cancers. The Colorectal Neoplasia Differentially Expressed (CRNDE) lncRNA is transcribed from chromosome 16 on the opposite strand to the neighboring IRX5 gene. It was originally discovered abnormally expressed in colorectal cancer (CRC) and was certified a critical biomarker in many cancers. However, its biological function and mechanism underlying the tumorigenesis of cervical cancer still require exploration. This study confirmed that CRNDE is markedly up-regulated in clinical tissues and cell lines of cervical cancer. The high expression of CRNDE positively correlates with advanced FIGO stage and lymph node metastasis. Furthermore, the overall survival rate in the group with highly expressed CRNDE was worse, and the high level of CRNDE may be regarded a prognostic factor because of its results from proportional hazard analysis. Loss-of-function assays revealed that CRNDE influences proliferation and apoptosis in cervical cancer cells, and Western blot assays revealed that the PI3K/AKT pathway was inactivated in response to CRNDE knockdown. Therefore, we conclude that CRNDE exerts oncogenic function in cervical cancer and should be further explored as a novel prognostic predictor.

Key words: lncRNA CRNDE, cervical cancer, proliferation, PI3K/AKT

Cervical cancer (CC) has been one of the most common global gynecological malignancies for several decades. Despite novel therapies and vaccination against human-papilloma virus HPV in younger women, the survival rate of cervical cancer patients is still dismal. Therefore, it is necessary to find novel therapeutic methods for CC patients and it is crucial to find potential therapeutic targets and establish the molecular mechanisms modulating CC progression.

Long noncoding RNAs (lncRNAs) are a group of RNA molecules longer than 200 t which have been verified as extremely significant in tumorigenesis [1–8]. The long non-coding RNA Colorectal Neoplasia Differentially Expressed (CRNDE) transcribed from chromosome 16 on the opposite strand to the neighboring IRX5 gene is the most up-regulated lncRNA in colorectal cancer [9]. It was originally identified to be aberrantly expressed in CRC [10] and other types of cancers, including HCC, ovarian, gallbladder and kidney cancers and glioma [11–16]. Although CRNDE has been a research focus in many types of cancers, its specific function in cervical cancer has not yet been fully

elucidated. It has been proven capable of promoting proliferation, metastasis, EMT progress and impedes apoptosis in all the above cancers. Additionally, high expression of CRNDE usually predicts poor prognosis. Many documents have reported that CRNDE is oncogenic, and based on the associated research, we studied the biological role of CRNDE in CC. It is speculated that the oncogenic functions of CRNDE are exerted in cancers so we examined the effects of CRNDE on CC biological activity.

The PI3K/AKT signaling pathway was proven important in the proliferation and metastasis of cancer cells [17]. Our literature research revealed that this is a classic pathway and significant for cancer research because it can promote progression and development of tumors. Once this signaling pathway was activated, the cancer cells would powerfully generate. The PI3K-AKT pathway function has been verified in many cancers, such as gallbladder carcinoma [15], gastric cancer [18] and thyroid cancer [19]. In this study, we tested the expression level of CRNDE in clinical tissues and cell lines by quantitative real-time PCR (qRT-PCR) The relation-

ship between CRNDE deregulation and clinical characteristics or prognosis was analyzed and functional assays indicated that silenced CRNDE weakened CC cell proliferation and prompted cell apoptosis. Mechanism experiments finally revealed that PI3K/AKT is related to CRNDE-mediated function in cervical cancer and findings revealed that CRNDE provides novel insights for exploring clinical treatment targets.

Materials and methods

The prognostic information and expression pattern of CRNDE in cervical cancer patients were downloaded from the TCGA database and analyzed by edger function.

Clinical samples. A total of 63 pairs of cervical cancer tissue samples and matched adjacent normal tissue samples were selected from patients who received surgery from 2008 to 2012 in the Gynecology, Second Hospital of Shandong University. No patients recruited in this study had received chemotherapy or radiotherapy. This study acquired approval of the Research Ethics Committee of the Second Hospital of Shandong University and all patients provided informed consent. All specimens were handled and made anonymous in accordance with the ethical and legal standards.

Cell culture and transfection. CC cells (C33A, CaSki, SiHa, and HeLa) and the normal human cervical epithelial cell line (H8) were obtained from the Type Culture Collection of the Chinese Academy of Sciences (Shanghai Institute of Biochemistry and Cell Biology, Shanghai, China). From these cells, HeLa and CaSki cell lines were maintained and cultured in RPMI 1640 medium (Gibco, Thermo Scientific, Waltham, MA) containing 10% of fetal bovine serum (FBS; Gibco). In addition, SiHa, C33A and H8 cells were preserved in Dulbecco's modified Eagle medium (Gibco) supplemented with 10% of FBS. All cells were maintained in a cell incubator with a humidified atmosphere (37 C and 5% CO_2).

To knock down CRNDE expression, siRNA specifically targeted CRNDE and the negative control siRNA (si-NC) were constructed by GenePharma Co. (Shanghai, China). The siRNA sequence is 5' UAUGGAAGCAUCACACUUAACACCU 3'; 5' GCUAUUGGAAGGAGGAGAUUCUGAA 3'. For colony formation assay, cells were transfected with CRNDE specific shRNA, sh-CRNDE and negative controls were bought from GenePharma Co. (Shanghai, China). The sequence of CRNDE was then sub-cloned into the pcDNA 3.1 vector and PcDNA-CRNDE accompanied with Lipofectamine 2000 (Invitrogen, Carlsbad, CA, USA) was used to over-express CRNDE in CC cells. Empty pcDNA vector was used as negative control (NC).

Quantitative real-time PCR (qRT-PCR). TRIzol reagent (Invitrogen) was isolated total RNA from CC specimens and cell lines. The PrimeScript RT reagent Kit (Takara Bio Company, Shiga, Japan) was then applied to synthesize the cDNA from 200 ng of previously extracted total RNA. The SYBR Green Kit (Takara Bio Company), cDNA was ampli-

fied by qRT-PCR in an ABI PRISM 7500 Sequence Detection System (Applied Biosystems). GAPDH was used as an internal control. In order to determine the relative quantification of gene expression levels, the $2^{-\Delta\Delta Ct}$ method was utilized. The sequences of all premiers were synthesized by RiboBio (Guangzhou, China) as shown in following: CRNDE, forward 5'-TGAAGGAAGGAAGTGGTGCA-3' and reverse 5'-TCCAGTGGCATCCTACAAGA-3'; GAPDH, forward 5'-TGCACCACCAACTGCTTAG-3' and reverse 5'-AGTAGAGGCAGGGATGATGTTC-3'. Each experiment was performed in triplicate.

Cell cytoplasm/nucleus fraction isolation. To extract cytoplasmic and nuclear fractions from CC cells, NE-PER Nuclear and Cytoplasmic Extraction Reagents (Thermo Scientific, Waltham, MA, USA) were employed. Then, qRT–PCR analysis was designed to examine the levels of lncRNA CRNDE in the nucleus and cytoplasm. U6 and GAPDH were used as positive and negative controls, separately.

MTT assay. Cells ($3\times10^3\sim6\times10^3$) were inoculated in a plate with 96 wells (200 μl per well, 6 repeated wells) at 37 °C and 5% CO_2 for one to three days. MTT solutions (20 μl, density: 5 mg/ml, Sigma) was gradually added to each well. After incubation for 4 h at 37 °C and 5% CO_2, this was stopped, and the culture medium was abandoned. DMSO (150 μl) (Sigma) added to each well and gently shaken for 10 min to promote the dissolution of crystallization. Absorbance values (OD) were measured by enzyme-linked immunosorbent detector at different time points (12 h, 24 h, 48 h, 72 h, 96 h). The experiment was in triplicate.

CCK-8 assay. CC cells (CaSki and HeLa) were transferred into the 96-well plates at 12 hour's post-transfection. 10l CCK-8 solution (Beyotime, Shanghai, China) was added to each cell at different time point (24, 48 and 72 hours) and absorbance was measured at 450 nm after the treated cells were incubated for 4 hours at 37°C.

Colony formation assay. We plated 500 cells/well in 6-well plates and incubated them in RPMI 1640 containing 10% FBS at 37 °C. After two weeks, cells were observed to be fixed and 0.1% of crystal violet stained these cells. Finally, we counted the number of visible colonies manually.

Flow cytometric analysis of apoptosis. After transfection for 48 hours with the indicated plasmid or negative control, the cells were harvested. Annexin V: FITC Apoptosis Detection Kits (BD Biosciences, USA), and flow cytometry detected the apoptosis rate. All samples were independently assayed in triplicate.

Western blot assay. Cells were lysed with RIPA (Thermo Scientific, USA) supplemented with protease inhibitors (Roche, Switzerland). Proteins (fifty micrograms) were separated by SDS-PAGE, followed by their transfer to PVDF membranes (Roche, Switzerland). The membranes were then blocked and incubated with rabbit anti-human cleaved caspase-3 antibody (1:1,000; 9661, CST, USA), cleaved PARP antibody (1:1,000; 5625, CST, USA), p-PI3K (1:1,000; 4228, CST, USA), PI3k antibody (1:1,000; 4249, CST, USA),

p-AKT (1:1,000; 4060, CST, USA), AKT antibody (1:1,000; 4685, CST, USA) at 4°C overnight. Membranes were then washed and probed by TBST and HRP Goat-anti-Rabbit (1:2000; sc-2040, Santa Cruz Biotechnology) independently at room temperature for 2 h. Finally, the protein levels were semi-quantitatively assessed by ECL (Thermo Scientific) and normalized to GAPDH (1:3,000; 5174, CST, USA).

Statistical analysis. SPSS 19.0 software (SPSS Inc., Chicago, IL, USA) analyzed samples. Data is shown as means ± standard deviation (SD). The Pearson χ^2 test evaluated the relationship between the expression of CRNDE and clinical-pathological factors, and comparison between two groups was by Student "t" test. Multiple comparisons were made by One-way ANOVA, and Kaplan-Meier survival analysis was performed. Differences among patient groups were compared by log-rank test and factors associated with the overall survival were identified by Cox regression model for multivariate survival analysis of cervical cancer. P-value less than 0.05 indicated statistical significance.

Results

CRNDE was significantly over-expressed in cervical cancer tissues and cell lines. In order to explore the biological functions of CRNDE in cervical cancer, we firstly examined the expression level of CRNDE in tissues (306 CC tissues and three normal tissues) obtained from the TCGA database (Supplementary Table 1). CRNDE was extremely up-regulated in CC tissues compared to normal tissues. To obtain further evidence, we measured the expression level of CRNDE in both 63 cervical cancer tissues and their corresponding normal tissues. As illustrated in Figure 1A, the level of CRNDE was significantly increased in cervical cancer tissues in comparison with that in the matched adjacent normal tissues.

We then measured the level of CRNDE in CC cell lines (SiHa, CasKi, HeLa and C33A) and a normal human cervical epithelial cell line (H8). As demonstrated in Figure 1B, compared with the normal human epithelial cell line, CRNDE was obviously up-regulated in cancerous cell lines, especially in the HeLa and CaSki cells which were selected for following experiments. These findings indicated that CRNDE could well be a cervical cancer oncogene.

The correlation between CRNDE level and CC clinical-pathological features. Pearson's χ^2 test clarified the relevance between CRNDE expression and clinical-pathological features of cervical cancer patients. Statistical results revealed that high CRNDE level was obviously correlated with FIGO stage (*p=0.045) and lymph node metastasis (**p<0.001) rather than with other clinical-pathological factors such as age, tumor size, histology and differentiation (Table 1; p>0.05) in terms of cervical cancer patients. These combined findings indicate that high level of CRNDE was closely related with cervical cancer progression. The gynecological oncology was divided into different stages in accordance with the specific pathological features. The standards for stage division were enacted by the International Federation of Gynecology and Obstetrics (FIGO) [20]. According to the specific biological features, patient samples used in this study were divided into stage Ib–IIa and stage IIb~IIIa groups.

High level of CRNDE predicted poor prognosis in cervical cancer patients. The mean value of CRNDE expression was taken as the cutoff value between high and low expression. 63 cervical cancer tissues were classified into two groups (Low: n=31; High: n=32) to further justify whether CRNDE expression had internal association with patient survival rate. In addition, the potential value of CRNDE was estimated for relevant clinical and pathological factors. Based on the Cox regression model, multivariate analysis established that high CRNDE level could be an independent
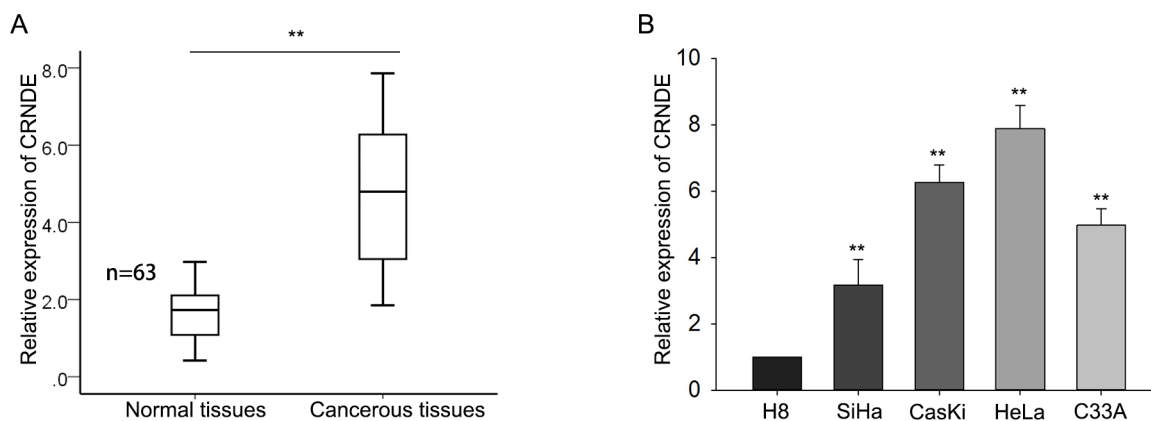

Figure 1. CRNDE was significantly over-expressed in CC tissues and cell lines. The level of CRNDE was clearly detected by qRT-PCR in CC tissues (A) and CC cells (B). Error bars represent means ± SD from at least three independent experiments were shown. **p<0.01.

prognostic factor in CC (Table 2, *p=0.036, **p=0.002). The result of the Kaplan-Meier analysis suggested that patients from the group with high CRNDE expression had markedly shorter overall survival than the low expression group (p<0.01, Figure 2A). All these results suggested that CRNDE be proposed as a potential biomarker for poor prognosis in cervical cancer. The survival curve downloaded from TCGA database also showed that high expression of CRNDE was positively correlated with the short survival time of CC patients (p=0.00206, Figure 2B).

Silenced CRNDE impaired cell proliferation and induced apoptosis in cervical cancer. We conducted cell cytoplasm/nucleus fraction isolation to assess if CRNDE regulated the biological activities of CC at post-transcriptional level, and found that CRNDE was located in the CC cell cytoplasm (Figure 3A). To better understand the effect

Table 1. Correlation between lncRNA-CRNDE expression and clinical features (n=63).

Variable	LncRNA-CRNDE Expression		p-value
	low	high	
Age			
<50	10	12	0.793
≥50	21	20	
Histologic type			
SCC	16	21	0.311
AD/ASC	15	11	
FIGO stage			
Ib–IIa	19	11	0.045*
IIb~IIIa	12	21	
Large Tumor Size			
<4	19	12	0.079
≥4	12	20	
Poor Differentiation			
Well+Moderate	23	16	0.070
Poor	8	16	
Lymph node metastasis			
Negative	26	9	<0.001**
Positive	5	23	

Low/high by the sample mean. Pearson χ^2 test. *p<0.05 was considered statistically significant.

Table 2. Multivariate and univariate analyses of prognostic parameters in patients with cervical cancer by Cox regression analysis.

Variable	Multivariate analysis			Univariate analysis		
		95% CI			95% CI	
	p-value	Low	High	p-value	Low	High
Age						
<50	0.808	0.491	1.741	0.926	0.544	1.729
≥50						
Histologic type						
SCC	0.222	0.349	1.277	0.12	0.36	1.124
AD/ASC						
FIGO stage						
Ib–IIa	0.761	0.569	2.161	0.365	0.744	2.231
IIb~IIIa						
Tumor Size (cm)						
<4	0.449	0.691	2.302	0.356	0.749	2.232
≥4						
Poor Differentiation						
Well+						
Moderate	0.127	0.272	1.176	0.645	0.651	2.000
Poor						
Lymph node metastasis						
Negative	0.013	1.244	6.140	0.003	1.341	4.054
Positive						
CRNDE level						
High	0.036**	0.263	0.957	0.002**	0.230	0.707
Low						

Cox regression analysis showed a positive, independent prognostic importance of CRNDE expression (p=0.036*, p=0.002**). *p<0.05 was considered statistically significant.
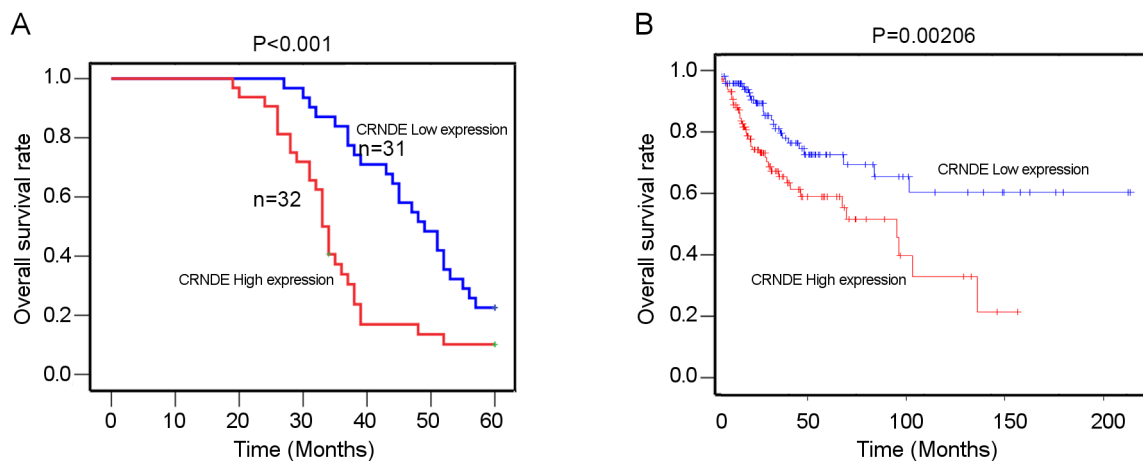

Figure 2. The relevance between CRNDE expression and overall survival for cervical cancer patients (A) was analyzed by means of Kaplan-Meier method analysis and TCGA database analysis (B). Error bars represent means ± SD from at least three independent experiments were shown. **p<0.01.
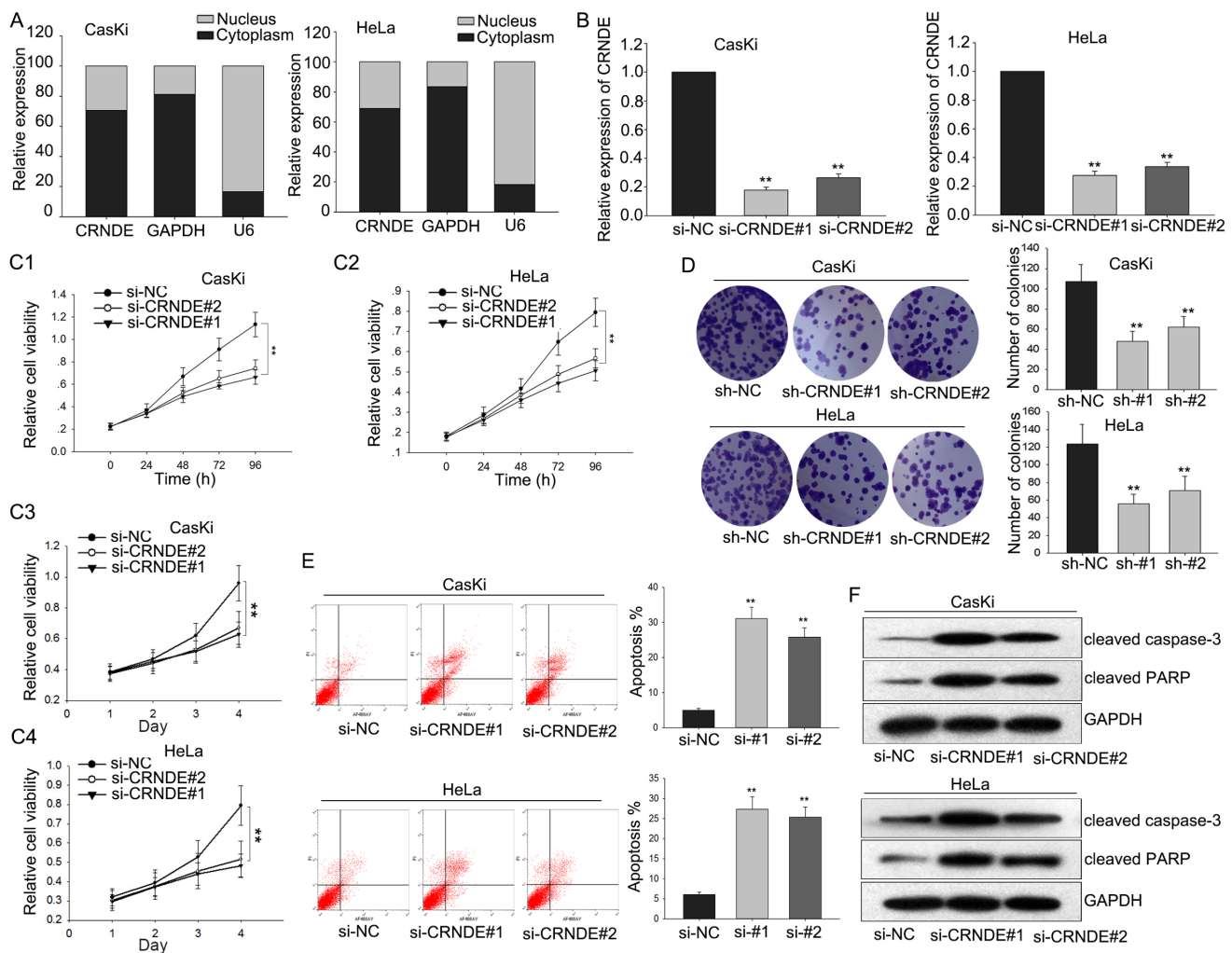
Figure 3. Silenced CRNDE impaired cell proliferation ability and induced apoptosis in cervical cancer. A) We tested the expression of CRNDE in cytoplasm or nucleus in CC cells. GAPDH and U6 were separately used as cytoplasmic marker and nuclear marker. B) Si-CRNDE transfection was performed in CaSki and HeLa cells. C) MTT assay and CCK-8 assay measured the influence of down-regulated CRNDE on the proliferation ability of two CC cells. D) The proliferation ability of CC cells was detected by colony formation assay after sh-CRNDE transfection. E) The effect of down-regulated CRNDE on the apoptosis of CaSki and HeLa cells was analyzed by flow cytometric analysis. F) Western blot assay was applied to examine the expressions of apoptosis-related proteins in response to silenced CRNDE. Error bars represent means ± SD from at least three independent experiments were shown. ** $p<0.01$.

of CRNDE on CC cells, we designed loss-of-function assays. Following transfection with siRNA, qRT-PCR analysis showed that CRNDE was observably down-regulated in both CaSki and HeLa cells compared to the si-NC group (Figure 3B). Results of MTT assay and CCK-8 assay revealed that decreased expression of CRNDE suppressed cell viability in the CaSki and HeLa cells (Figure 3C). Similarly, colony formation assay demonstrated the inhibitory effect of silenced CRNDE on cell proliferation ability (Figure 3D) and flow cytometry analysis established increased apoptosis rate in CRNDE-silenced CC cells (Figure 3E). Moreover, the levels of proteins related to apoptosis (cleaved caspase-3 and cleaved PARP) were also increased when CRNDE was

silenced (Figure 3F). These combined results suggest that CRNDE acts as a tumor promoter in cell proliferation and inhibits cell apoptosis in cervical cancer.

Knockdown of CRNDE inactivated the PI3K/AKT pathway in cervical cancer. The PI3K/AKT pathway had been identified to be deregulated in tumorigenesis, therefore we hypothesized that the PI3K/AKT pathway participates in CRNDE-mediated biological regulation in CC cells. To prove this, we applied western blot analysis to measure the levels of phosphorylated PI3K (p-PI3K), and AKT (p-AKT) in two CC cells in response to silenced CRNDE. As shown in Figure 4A, silenced CRNDE reduced p-PI3K and p-AKT levels in HeLa cells. We therefore concluded that the PI3K/

AKT pathway is involved in CRNDE-mediated function in cervical cancer cells.

CENDE promoted CC proliferation and inhibited apoptosis by targeting PI3K/AKT. We designed and performed rescue assays in HeLa cells to demonstrate the positive influence of CRNDE on CC progression. This revealed that CRNDE was up-regulated in HeLa cells (Figure 5A), so we then measured cell proliferation in the CRNDE-over-expressed CC cells by MTT, CCK-8 and colony formation assays (Figures 5B–D). The results showed that over-expression of CRNDE inhibited cell apoptosis.

LY94002 is an effective inhibitor of the PI3K-AKT signaling pathway [21]. We added this to the CRNDE-up-regulated HeLa cells and the inactivated PI3K-AKT signaling pathway reversed the increased cell proliferation. Our flow cytometry and Western blot analyses then detected cell apoptosis (Figures 5E–F), and results confirmed that the decreased apoptotic rate of CRNDE-over-expressed HeLa cells is enhanced by LY94002 supplement. The combined results enabled the conclusion that CRNDE promotes cell proliferation and suppresses cell apoptosis in cervical cancer through modulation of the PI3K-AKT signaling pathway.

Discussion

It has been revealed that almost 97% of the human genome sequence is transcribed into non-coding RNAs (ncRNAs), and long noncoding RNAs (lncRNAs) are proposed as valuable novel molecules because they are deregulated in many cancers [8, 22–24]. For example, Zhang R et al. certified that lncRNA TP73-AS1 interacts with miR-142, thus modulating cell growth in brain glioma by activating the HMGB1/RAGE pathway [17].

Ye K et al. previously proved that lncRNA GAS5 negatively affected cell growth and reversed epithelial-mesenchymal transition in osteosarcoma by modulating the miR-221/ARHI pathway [25]. And Ma F et al. revealed that lncRNA TUG1 accelerated proliferation and metastasis in gallbladder carcinoma cells by negatively manipulating miR-300 [26].

Many other lncRNAs were also identified to exert critical biological functions in cervical cancer. For example, lncRNA PVT1 epigenetically silences miR-195, thus affecting EMT and chemo-resistance in cervical cancer cells [27]. Further, LncRNA HOXA11 antisense motivates the progression and maintenance of stem cells in cervical cancer [28], and
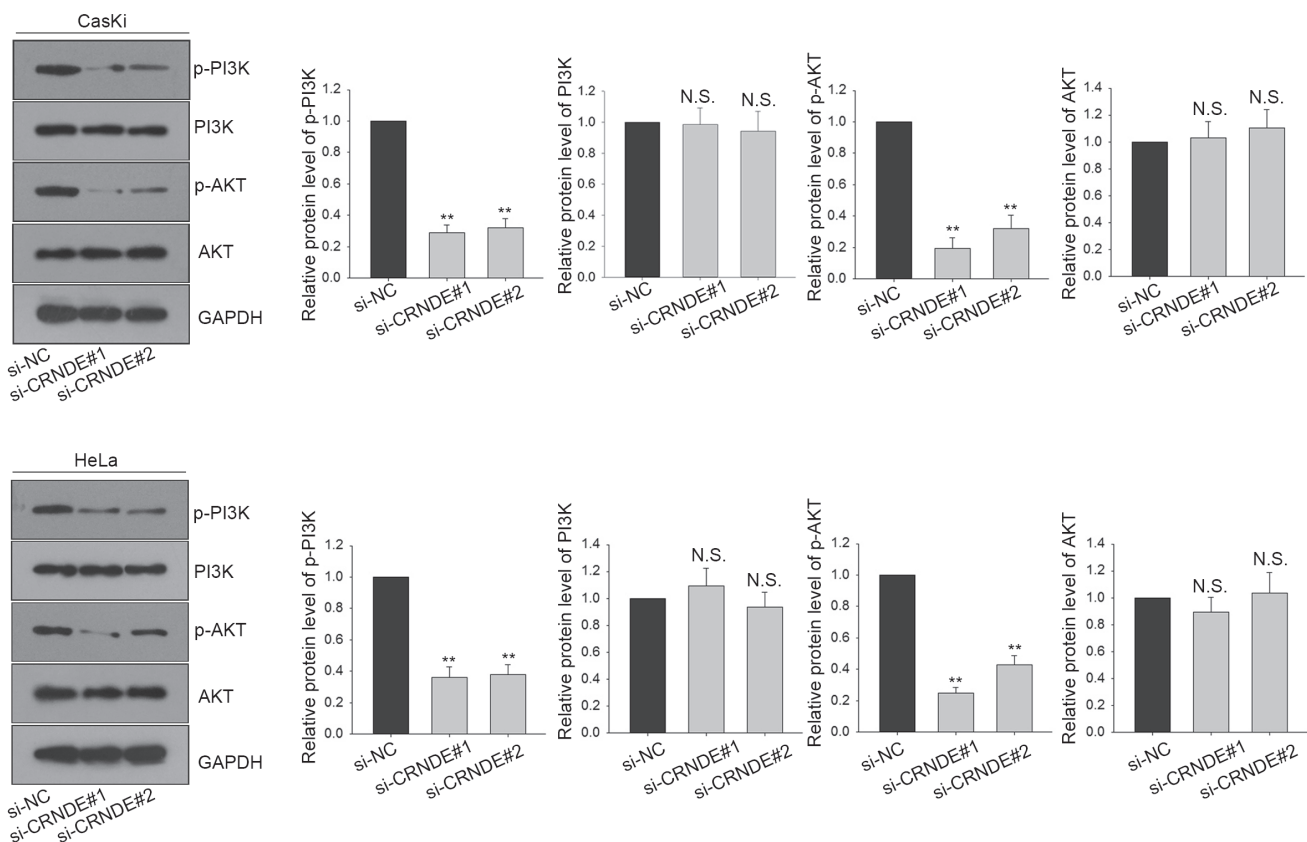

Figure 4. Knockdown of CRNDE inactivated the PI3K/AKT pathway in cervical cancer. Western blot assay was conducted to measure the levels of p-PI3K, PI3K, p-AKT and AKT in two CC cells in response to silenced CRNDE. Error bars represent means ± SD from at least three independent experiments were shown. ** p<0.01.
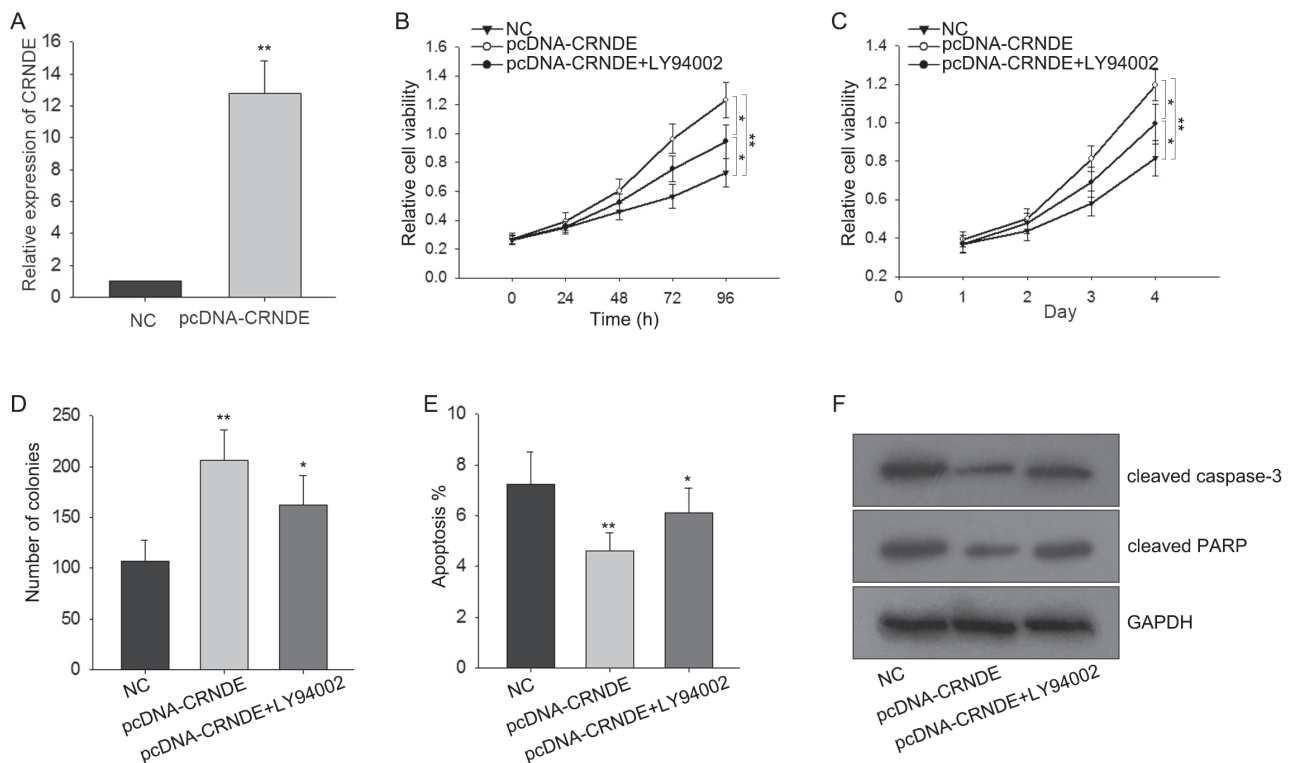
Figure 5. CENDE promoting proliferation and inhibiting apoptosis of cervical cancer cells through targeting PI3K/AKT. A) CRNDE was upregulated in HeLa cells by transfection of pcDNA-CRNDE. Cell proliferation was examined by MTT (B), CCK-8 (C) and colony formation assays (D) after HeLa cell was co-transfected with pcDNA-CRNDE and LY94002. E) Flow cytometry analysis investigated the influence of pcDNA-CRNDE and LY94002 on HeLa cell apoptosis. F) The apoptosis condition of HeLa cell was measured by western blot analysis through measuring the apoptotic proteins. Error bars represent means ± SD from at least three independent experiments were shown. **p<0.01.

lncRNA ANRIL forecasts poor prognosis of cervical cancer and further stimulates carcinogenesis through the PI3K/AKT pathways [29]. Despite this research, there are still many unknown lncRNAs requiring investigation.

LncRNA Colorectal Neoplasia Differentially Expressed (CRNDE), which was transcribed from chromosome 16 on the strand opposite to the contiguous IRX5 gene, was originally found up-regulated in CRC and then reported to be abnormally expressed in many other cancers [10, 12, 16, 30]. However, its potential role and molecular mechanisms in cervical cancer remain unclear. In addition to all of the above reports, CRNDE can act as an oncogene to affect EMT formation, cell growth, metastasis and other processes through interaction with the PI3K/AKT signaling pathway. For example, CRNDE exerts oncogenic function in gallbladder carcinoma through the PI3K/AKT signaling pathway [15], and therefore it is proposed that CRNDE can interact with this pathway to promote cancer progression.

Herein, we demonstrated that CRNDE was significantly up-regulated in CC tissues and cells, and its increased expression is obviously associated with FIGO stages, lymph node metastasis and closely correlated with poor prognosis in cervical cancer patients. Loss-of-function assays then demonstrated that CRNDE knockdown significantly inhib-

ited CC cell proliferation and increased their apoptosis. Further mechanism experiments revealed that PI3K/AKT is involved in CRNDE-mediated CC function, and our next study will focus on the mechanism of CRNDE mechanisms in regulating cervical cancer cells.

In conclusion, we demonstrated that CRNDE was certainly up-regulated in cervical cancer cell lines and tissues and was closely correlated with poor prognosis in cervical cancer patients. The cellular assays proved that CRNDE participates in multiple CC processes, and the combined results imply that CRNDE should be a successful candidate as both a prognostic biomarker and target in cervical cancer treatment.

Supplementary information is available in the online version of the paper.

Acknowledgments: The authors thank the laboratory members.

References

[1]   ZHANG CL, ZHU KP, MA XL. Antisense lncRNA FOXC2-AS1 promotes doxorubicin resistance in osteosarcoma by increasing the expression of FOXC2. Cancer Lett 2017. 396: 66–75. https://doi.org/10.1016/j.canlet.2017.03.018

[2]   YU H, XUE Y, WANG P, LIU X, MA J et al. Knockdown of long non-coding RNA XIST increases blood-tumor barrier permeability and inhibits glioma angiogenesis by targeting miR-137. Oncogenesis 2017; 6: e303. https://doi.org/10.1038/oncsis.2017.7

[3]   YANG R, LI P, ZHANG G, LU C, WANG H et al. Long Non-Coding RNA XLOC_008466 Functions as an Oncogene in Human Non-Small Cell Lung Cancer by Targeting miR-874. Cell Physiol Biochem 2017; 42: 126–136. https://doi.org/10.1159/000477121

[4]   XUE Y, NI T, JIANG Y, LI Y. Long Noncoding RNA GAS5 Inhibits Tumorigenesis and Enhances Radiosensitivity By Suppressing miR-135b Expression in Non-Small Cell Lung Cancer. Oncol Res 2017; 25: 1305–1316. https://doi.org/10.3727/096504017X14850182723737

[5]   XU J, ZHANG R, ZHAO J. The Novel Long Noncoding RNA TUSC7 Inhibits Proliferation by Sponging MiR-211 in Colorectal Cancer. Cell Physiol Biochem 2017; 41: 635–644. https://doi.org/10.1159/000457938

[6]   XIONG H, NI Z, HE J, JIANG S, LI X et al. LncRNA HULC triggers autophagy via stabilizing Sirt1 and attenuates the chemosensitivity of HCC cells. Oncogene 2017; 36: 3528–3540. https://doi.org/10.1038/onc.2016.521

[7]   XIAO JN, YAN TH, YU RM, GAO Y, ZENG WL et al. Long non-coding RNA UCA1 regulates the expression of Snail2 by miR-203 to promote hepatocellular carcinoma progression. J Cancer Res Clin Oncol 2017;143: 981–990. https://doi.org/10.1007/s00432-017-2370-1

[8]   XIA M, YAO L, ZHANG Q, WANG F, MEI H et al. Long noncoding RNA HOTAIR promotes metastasis of renal cell carcinoma by up-regulating histone H3K27 demethylase JMJD3. Oncotarget 2017; 8: 19795–19802. https://doi.org/10.18632/oncotarget.15047

[9]   LIU T, ZHANG X, YANG YM, DU LT, WANG CX. Increased expression of the long noncoding RNA CRNDE-h indicates a poor prognosis in colorectal cancer, and is positively correlated with IRX5 mRNA expression. Onco Targets Ther 2016; 9: 1437–1448. https://doi.org/10.2147/OTT.S98268

[10] GRAHAM LD, PEDERSEN SK, BROWN GS, HO T, KASSIR Z et al. Colorectal Neoplasia Differentially Expressed (CRNDE), a Novel Gene with Elevated Expression in Colorectal Adenomas and Adenocarcinomas. Genes Cancer 2011; 2: 829–840. https://doi.org/10.1177/1947601911431081

[11] CHEN Z, YU C, ZHAN L, PAN Y, CHEN L et al. LncRNA CRNDE promotes hepatic carcinoma cell proliferation, migration and invasion by suppressing miR-384. Am J Cancer Res 2016; 6: 2299–2309.

[12] DONG R, LIU XQ, ZHANG BB, LIU BH, ZHENG S et al. Long non-coding RNA-CRNDE: a novel regulator of tumor growth and angiogenesis in hepatoblastoma. Oncotarget 2017; 8: 42087–42097. https://doi.org/10.18632/oncotarget.14992

[13] JING SY, LU YY, YANG JK, DENG WY, ZHOU Q et al. Expression of long non-coding RNA CRNDE in glioma and its correlation with tumor progression and patient survival. Eur Rev Med Pharmacol Sci 2016; 20: 3992–3996.

[14] SHAO K, SHI T, YANG Y, WANG X, XU D et al. Highly expressed lncRNA CRNDE promotes cell proliferation through Wnt/beta-catenin signaling in renal cell carcinoma. Tumour Biol 2016. https://doi.org/10.1007/s13277-016-5440-0

[15] SHEN S, LIU H, WANG Y, WANG J, NI X et al. Long noncoding RNA CRNDE promotes gallbladder carcinoma carcinogenesis and as a scaffold of DMBT1 and C-IAP1 complexes to activating PI3K-AKT pathway. Oncotarget 2016; 7: 72833–72844. https://doi.org/10.18632/oncotarget.12023

[16] SZAFRON LM, BALCERAK A, GRZYBOWSKA EA, PIENKOWSKA-GRELA B, PODGORSKA A et al. The putative oncogene, CRNDE, is a negative prognostic factor in ovarian cancer patients. Oncotarget 2015; 6: 43897–43910. https://doi.org/10.18632/oncotarget.6016

[17] YIN K, WANG L, ZHANG X, HE Z, XIA Y et al. Netrin-1 promotes gastric cancer cell proliferation and invasion via the receptor neogenin through PI3K/AKT signaling pathway. Oncotarget 2017; 8: 51177–51189. https://doi.org/10.18632/oncotarget.17750

[18] YE J, HUANG J, XU J, HUANG Q, WANG J et al. ERp29 controls invasion and metastasis of gastric carcinoma by inhibition of epithelial-mesenchymal transition via PI3K/Akt-signaling pathway. BMC Cancer 2017; 17: 626. https://doi.org/10.1186/s12885-017-3613-x

[19] WANG SC, CHAI DS, CHEN CB, WANG ZY, WANG L. HPIP promotes thyroid cancer cell growth, migration and EMT through activating PI3K/AKT signaling pathway. Biomed Pharmacother 2015; 75: 33–39. https://doi.org/10.1016/j.biopha.2015.08.027

[20] JUNG W, PARK KR, LEE KJ, KIM K, LEE J et al. Value of imaging study in predicting pelvic lymph node metastases of uterine cervical cancer. Radiat Oncol J 2017; 35: 340–348. https://doi.org/10.3857/roj.2017.00206

[21] FENG Y, ZU LL, ZHANG L. MicroRNA-26b inhibits the tumor growth of human liver cancer through the PI3K/Akt and NF-kappaB/MMP-9/VEGF pathways. Oncol Rep 2018; 39: 2288–2296. https://doi.org/10.3892/or.2018.6289

[22] ZHU M, LIU J, XIAO J, YANG L, CAI M et al. Lnc-mg is a long non-coding RNA that promotes myogenesis. Nat Commun 2017; 8: 14718. https://doi.org/10.1038/ncomms14718

[23] ZHANG CZ. Long non-coding RNA FTH1P3 facilitates oral squamous cell carcinoma progression by acting as a molecular sponge of miR-224-5p to modulate fizzled 5 expression. Gene 2017; 607: 47–55. https://doi.org/10.1016/j.gene.2017.01.009

[24] XIA S, JI R, ZHAN W. Long noncoding RNA papillary thyroid carcinoma susceptibility candidate 3 (PTCSC3) inhibits proliferation and invasion of glioma cells by suppressing the Wnt/beta-catenin signaling pathway. BMC Neurol 2017; 17: 30. https://doi.org/10.1186/s12883-017-0813-6

[25] YE K, WANG S, ZHANG H, HAN H, MA B et al. Long noncoding RNA GAS5 suppresses cell growth and epithelial-mesenchymal transition in osteosarcoma by regulating the miR-221/ARHI pathway. J Cell Biochem 2017; 118: 4772–4781. https://doi.org/10.1002/jcb.26145

[26]   MA F, WANG SH, CAI Q, JIN LY, ZHOU D et al. Long non-coding RNA TUG1 promotes cell proliferation and metastasis by negatively regulating miR-300 in gallbladder carcinoma. Biomed Pharmacother 2017; 88: 863–869. https://doi.org/10.1016/j.biopha.2017.01.150

[27]   SHEN CJ, CHENG YM, WANG CL. LncRNA PVT1 epigenetically silences miR-195 and modulates EMT and chemoresistance in cervical cancer cells. J Drug Target 2017; 25: 637–644. https://doi.org/10.1080/1061186X.2017.1307379

[28]   KIM HJ, EOH KJ, KIM LK, NAM EJ, YOON SO et al. The long noncoding RNA HOXA11 antisense induces tumor progression and stemness maintenance in cervical cancer. Oncotarget 2016; 7: 83001–83016. https://doi.org/10.18632/oncotarget.12863

[29]   ZHANG D, SUN G, ZHANG H, TIAN J, LI Y. Long noncoding RNA ANRIL indicates a poor prognosis of cervical cancer and promotes carcinogenesis via PI3K/Akt pathways. Biomed Pharmacother 2017; 85: 511–516. https://doi.org/10.1016/j.biopha.2016.11.058

[30]   LIU T, ZHANG X, GAO S, JING F, YANG Y et al. Exosomal long noncoding RNA CRNDE-h as a novel serum-based biomarker for diagnosis and prognosis of colorectal cancer. Oncotarget 2016; 7: 85551–85563. https://doi.org/10.18632/oncotarget.13465

	CRNDE
normal	107,3966786
normal	160,5443433
normal	161,5507771
tumor	74,21251916
tumor	1103,872679
tumor	1011,889115
tumor	273,4128674
tumor	633,8547494
tumor	27,62760588
tumor	67,37949853
tumor	1006,339849
tumor	1334,155171
tumor	905,0847685
tumor	424,5145913
tumor	556,1034845
tumor	1256,404795
tumor	286,987434
tumor	1633,030507
tumor	32,61966104
tumor	338,0057515
tumor	717,4761551
tumor	936,2793411
tumor	437,570312
tumor	220,8428426
tumor	125,2022562
tumor	903,6390586
tumor	1339,344532
tumor	1503,843881
tumor	335,3098486
tumor	600,8249719
tumor	1107,700388
tumor	1580,927796
tumor	651,0630041
tumor	858,1838364
tumor	916,4337815
tumor	730,1981488
tumor	901,2548198
tumor	903,5455715
tumor	1885,20465
tumor	666,7984009
tumor	580,5147026
tumor	712,428023
tumor	1115,539848
tumor	856,9020562
tumor	339,7658332
tumor	713,4074851
tumor	282,3537049
tumor	2100,033774
tumor	134,9976078

tumor	422,8103515
tumor	804,1729719
tumor	2,933325676
tumor	1137,561811
tumor	784,9123571
tumor	1310,202068
tumor	657,4030021
tumor	584,5390423
tumor	762,4199259
tumor	200,1889723
tumor	1389,082711
tumor	984,907891
tumor	815,8202835
tumor	482,2119158
tumor	814,9838996
tumor	1299,072346
tumor	1246,807091
tumor	1332,133632
tumor	1406,395742
tumor	2595,449006
tumor	862,6000683
tumor	1298,5035
tumor	1252,273436
tumor	839,8818538
tumor	1068,45658
tumor	1727,642396
tumor	685,3366676
tumor	1046,699947
tumor	1706,271909
tumor	1111,863151
tumor	697,0816905
tumor	662,4148369
tumor	819,7991427
tumor	831,2758036
tumor	1253,434546
tumor	608,4631462
tumor	1322,678413
tumor	1643,910343
tumor	556,7594853
tumor	1484,133473
tumor	1209,478385
tumor	873,4436749
tumor	490,5945446
tumor	2102,550988
tumor	1051,097968
tumor	1089,676009
tumor	799,6373606
tumor	29,43186664
tumor	417,3420315
tumor	769,6261582

tumor	1000,738377
tumor	876,5064481
tumor	570,1899267
tumor	1247,849932
tumor	27,17217877
tumor	1161,42568
tumor	2054,829891
tumor	600,8102399
tumor	2149,730912
tumor	1039,024806
tumor	1239,782994
tumor	1029,194542
tumor	1250,110926
tumor	1155,985003
tumor	707,9484532
tumor	1112,537274
tumor	1333,849861
tumor	361,3147581
tumor	858,2672973
tumor	562,7245282
tumor	70,50874102
tumor	2611,519783
tumor	1107,779478
tumor	1034,340728
tumor	1261,549082
tumor	2591,551963
tumor	560,9691816
tumor	1851,53898
tumor	1037,921644
tumor	924,3960218
tumor	676,128036
tumor	1629,340036
tumor	394,2056602
tumor	797,3012899
tumor	1952,369816
tumor	1495,762579
tumor	729,9364738
tumor	948,3045826
tumor	165,1500582
tumor	846,0996579
tumor	1386,657683
tumor	1273,729843
tumor	1096,699982
tumor	582,0346558
tumor	1363,595817
tumor	1418,220624
tumor	1030,422016
tumor	1097,89899
tumor	803,6144412
tumor	262,2814846

tumor	578,324303
tumor	1155,781429
tumor	194,0490131
tumor	1192,678497
tumor	670,261168
tumor	2514,728645
tumor	603,3536821
tumor	1244,878199
tumor	1142,00311
tumor	824,3419256
tumor	1241,031542
tumor	689,0241921
tumor	390,0235501
tumor	134,7739204
tumor	590,1310007
tumor	1551,019516
tumor	634,0370066
tumor	872,5563642
tumor	1731,11503
tumor	1181,477643
tumor	1291,305471
tumor	1849,344088
tumor	1429,217344
tumor	1691,025765
tumor	1240,161176
tumor	1013,29742
tumor	932,8857983
tumor	688,7656288
tumor	1451,557458
tumor	24,47670872
tumor	1544,284767
tumor	449,7124578
tumor	996,315827
tumor	1000,812201
tumor	933,7271427
tumor	2716,12742
tumor	793,3377868
tumor	2085,82028
tumor	938,8864299
tumor	846,3244644
tumor	450,0697891
tumor	1138,822134
tumor	2337,051949
tumor	440,4575728
tumor	859,6111084
tumor	1626,469825
tumor	585,0776367
tumor	214,5610955
tumor	1414,661706
tumor	1311,99436

tumor	1928,787657
tumor	1220,974582
tumor	1771,608287
tumor	350,9967748
tumor	641,486963
tumor	1337,858899
tumor	1878,315636
tumor	760,7703439
tumor	261,5593467
tumor	1396,464207
tumor	920,4159117
tumor	762,3211634
tumor	47,13945615
tumor	1005,033158
tumor	32,19749126
tumor	2047,979556
tumor	763,4831701
tumor	1266,999859
tumor	1548,370781
tumor	1210,944218
tumor	42,12259575
tumor	1364,603265
tumor	956,7745198
tumor	875,7062213
tumor	1775,980367
tumor	1436,018317
tumor	2220,353086
tumor	1004,47182
tumor	933,3757914
tumor	1269,806728
tumor	885,6855516
tumor	889,5422033
tumor	770,5243014
tumor	1876,535845
tumor	548,409031
tumor	1335,45377
tumor	2043,45523
tumor	3534,867224
tumor	72,45099307
tumor	1192,003792
tumor	929,891154
tumor	1730,920381
tumor	445,2256016
tumor	1182,137805
tumor	334,9441485
tumor	567,381588
tumor	1053,047768
tumor	2065,003506
tumor	763,4878508
tumor	1410,024634

tumor	797,989319
tumor	698,4418976
tumor	929,8511135
tumor	362,0700608
tumor	687,9834998
tumor	1297,954502
tumor	855,5663002
tumor	473,9689051
tumor	1193,162547
tumor	1062,265062
tumor	495,2289142
tumor	1045,516939
tumor	850,5483294
tumor	1065,010754
tumor	1042,782686
tumor	1996,295655
tumor	1778,393541
tumor	243,4249964
tumor	1994,110271
tumor	50,98234898
tumor	3566,922106
tumor	300,0431203
tumor	2071,429442
tumor	1682,365009
tumor	832,2537988
tumor	657,9734344
tumor	1388,824591
tumor	740,6674298
tumor	973,549192
tumor	704,4505619
tumor	441,5509903
tumor	1352,716672
tumor	1246,432737
tumor	750,7599559
tumor	1274,404138
tumor	646,8105132
tumor	1561,239866
tumor	1301,821871
tumor	2206,893389
tumor	689,7151061
tumor	521,9085891
tumor	480,3217841
tumor	304,1867999
tumor	715,4286406
tumor	1045,644278
tumor	1389,647075
tumor	1081,75478
tumor	1004,116347
tumor	1170,906145
tumor	2241,957675

tumor	1115,625889
tumor	352,6922191
tumor	741,4827554
tumor	252,3728166
tumor	781,1592475
tumor	1208,313628
tumor	2038,086377
tumor	1486,106806
tumor	915,3334469
tumor	1365,440341